ISSN 2278-2540 | DOI: 10.51583/IJLTEMAS | Volume XV, Issue V, May 2026

Impact of Dilution Air Flow Rate Modulation on Exit Temperature of Gas Turbine Combustion Chamber

Ephraim R. Afia[1]*; Felix N. Akam[2]; Nsikakabasi I. Bassey[3]; Philip E. Philip[4]; Immanuel H. Usoro[5]

[1,3]Department of Mechanical Engineering, Federal University of Technology, Ikot Abasi (FUTIA) Akwa Ibom State, Nigeria.

[2]Department of Marine Engineering, Akwa Ibom State University, Ikot Akpaden, Akwa Ibom State, Nigeria.

[4]Department of Mechanical Engineering, Nnamdi Azikiwe University, Awka, Anambra State, Nigeria.

[5]Department of Electrical Engineering, Federal University of Technology, Ikot Abasi (FUTIA) Akwa Ibom State, Nigeria.

***Corresponding Author**

DOI: https://doi.org/10.51583/IJLTEMAS.2026.150500053

Received: 01 May 2026; Accepted: 06 May 2026; Published: 28 May 2026

ABSTRACT

The management of exit temperature in gas turbine combustors is critical for ensuring turbine blade life, thermal efficiency, and operational flexibility. Dilution air injection is a primary method for cooling combustion products, yet the quantitative effect of modulating its flow rate on exit temperature remains insufficiently understood. This study employs a Computational Fluid Dynamics (CFD) approach using ANSYS FLUENT to investigate the impact of dilution air flow rate modulation on the exit temperature of a can-type gas turbine combustion chamber operating under steady-state conditions with methane fuel. A three-dimensional model of the combustor was developed, and simulations were performed for dilution air mass flow rates ranging from 0.001 kg/s to 0.005 kg/s. Results show a strictly monotonic decrease in exit temperature with increasing dilution air flow, yielding a total reduction of 87 °C (approximately 4.0%) across the tested range. However, diminishing marginal cooling effectiveness is observed, with the largest reduction (43 °C) occurring between 0.001kg/s and 0.002 kg/s and progressively smaller reductions at higher flow rates. The midpoint exit temperature decreases by about 20 °C when dilution air is increased from 100% to 400% of baseline. The study quantitatively demonstrates that while increased dilution air flow significantly reduces thermal loading, benefits diminish beyond an optimal range (approximately 0.003–0.004 kg/s or a 200–250% increase). These findings provide design engineers with quantitative criteria for balancing exit temperature reduction against pressure loss, combustion efficiency, and flame stability.

Keywords: Gas Turbine Combustor, Dilution Air Flow Rate, Exit Temperature, Modulation, CFD Simulation, Can-Type Combustor, Thermal Efficiency.

INTRODUCTION

The need to strike a balance between environmental regulations and demand for higher thermal efficiency and flexibility of operations possess a critical challenge for the operational management of modern gas turbine power plants[1-3] Critical to this challenge is the management of the exit temperature profile of the gas turbine combustion chamber; a critical component of the power plant arrangement that influences the life, efficiency

ISSN 2278-2540 | DOI: 10.51583/IJLTEMAS | Volume XV, Issue V, May 2026

and performance of other power plants components. Dilution air injection remains one of the primary means for reducing the internal and exit temperature of the gas turbine combustion chambers to an acceptable limit suitable for the turbine's blades, inlet nozzles and other auxiliary components. However, modulating it rate of flow to achieve a dynamic control of the exit temperature introduces a fundamental instability challenge. Specifically, poor or unsystematic modulation can lead to excessive and non-uniform thermal gradient in and at the exit combustor of the gas turbine power plant [1,4-6]. Also, the lack of understanding of the relationship between dilution air flow rate and temperature at the exit possess another challenge to design engineers and operators of the gas turbine power plants.

In the context of gas turbine combustor, dilution air refers to the secondary air flow introduced downstream of the primary combustor zone, designed to mix with and cool the hot expanding gases inside the combustor [2,7-8]. The dilution air does not participate in the exothermic reactions. The exit temperature profile, often defined by the dimensionless pattern factor is the spatial distribution of gas temperatures at the combustor – turbine interface [9-11]. On the other hand, modulation of the dilution flow rate refers to the process of using control mechanisms to alter the mass flow rate of air passing via the primary zone [12-16]. Extant literature reveals significant but fragmented progress. Early foundational study by [17] worked on improving the outlet temperature distribution of a dual fuel gas turbine combustor using a simplified CFD. Another work by [18] carried out numerical investigation on the effect of Dome cooling Air and emission behavior in a can type gas turbine and the cooling characteristics of dilution holes in can type combustor of a micro-gas turbine.[5] carried out a numerical simulation on effect of cooling hole diameter on the outlet temperature distribution of a gas turbine while [4] carried out an experimental study of fuel-air mixing and dilution jets on outlet temperature distribution on a small gas turbine combustor. Furthermore, a work by [19] looked at the influence of dilution and effusion flows in generating variable inlet profiles for high pressure turbine. A work by [20] studied the effects of methane mass flow rate variation on thermal field of the can type combustion chamber. Another work by [13] underscored numerical simulation on the effect of swirler installation angle on outlet temperature distribution in gas turbine. Also, [21] and [22] carried at a study on the effects of transient inlet air pressure of a gas turbine combustor exhaust emissions and the impact of secondary Air flow on combustor emissions respectively.

Despite the extensive body of research on this area, a significant gap remains in the quantitative understanding of how modulation of the dilution air flow rate affects the exit temperature of gas turbine combustors. This study seeks to quantify the relationship between the dilution air flow rate and the exit temperature of a can-type gas turbine combustor under steady-state conditions, employing a CFD approach. The results of this investigation are expected to facilitate the design of more efficient and thermally stable gas turbine combustion chambers.

MATERIALS AND METHOD

Materials

Combustion Chamber Material

The super-alloy Inconel 718, which is based on nickel, was selected as the material for the combustion chamber wall because of its exceptional strength and ability to withstand oxidation and corrosion at high temperatures.

Fluid Dynamics Computational Tool

In this study, CFD is utilized for analysis and simulation. During the research process, all relevant boundary conditions and assumptions were taken into consideration.

ISSN 2278-2540 | DOI: 10.51583/IJLTEMAS | Volume XV, Issue V, May 2026

Use of AutoCAD software

The combustion chamber under consideration was designed using the AutoCAD software.

Data Source and Gathering

The Ibom Power Plant Company, situated in the Ikot Abasi Local Government Area of Akwa Ibom State, Nigeria, provided some data for this study. Data are also obtained from published papers, experimental data from other researchers, and data bases or data logbooks.

Methods

Creating a 3D Model of the Combustion Chamber Geometry:

The Can type combustion chamber design was chosen for this study. Figure 1 shows the 3D geometry of the gas turbine Can-Type combustor chamber. The combustor's dimensions are 220 mm in diameter and 420 mm in the Z direction. Vanes give a whirling velocity component by directing the primary input air. The primary main air inlet has a total surface area of 80 cm^2. Fuel is introduced into the primary air flow by means of fuel inlets, each of which has a surface area of 0.21 cm^2. Twelve port air inlets, each with an area of 1.8 cm^2, are used to introduce the primary air into the combustion chamber. The unburned fuel is completely burned by injecting the secondary air after the primary air. The fuel injector injects 0.2 m of dilution air to regulate the flame temperature and NOx emissions. 0.05 m^2 is the area of the can-type combustor's circular outlet.

The CFD model used in this work considers a single Can. This system is composed of the primary burner, combustor wall, secondary air inlet, swirl air inlet, dilution air inlet, and output. Air and natural gas can enter the combustor through a swirl burner. Dilution air has two purposes, providing the additional air required for complete combustion and cooling the combustion liner, which is normally heated to a high temperature. It is directed to the surrounding cylinder concurrently with secondary air. To accurately depict the swirl flow prior to fuel-air mixing in the main primary zone, a swirl burner is also modeled. The liner holes are required to cool the combustion products, to maintain a constant temperature profile at the exit in the dilution zone, and to cool the liner wall configuration. They are also required to supply enough air to the primary zone for full combustion at the selected primary zone equivalency ratio of 1:2. The diameter of the air entrance holes is determined by the required greatest penetration. The effective sizes of the holes were calculated using the following formulae:

$$\frac{\Delta P3-4}{P3} = \frac{143.5 M_h \, T3}{P3^2 \, Cd^2 Ah^2} \quad (1)$$

$$Cd = \frac{k-1}{0.6\sqrt{[4k-k(2-\beta)^2]}} \quad (2)$$

$$k = 1 + 0.64\sqrt{[2\mu^2 + (4\mu^4 + 1.56\mu^2\,(4\beta - \beta^2)]} \quad (3)$$

Where:

Ah is the area of inlet ports.

$\frac{\Delta P3-4}{P3}$ term is taken to be 6%

Cd is given as 0.65.

ISSN 2278-2540 | DOI: 10.51583/IJLTEMAS | Volume XV, Issue V, May 2026

M_h denotes the mass flow rate through the ports (kg/s)

Solid Works, a modeling program, is used to model the combustor in 3-Dimensions. The end view of a 3D model of the Can Type combustion chamber is displayed in Figure 2. As seen in Figure 3, a reduced 2-Dimensional solid model was built and used to produce the computational grid (Meshed) in order to simplify the simulation and cut down on computing time as shown in Figure 4.

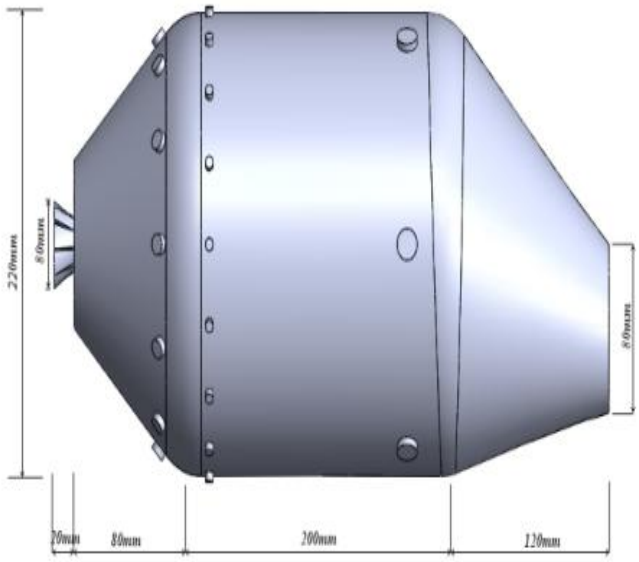

Figure 1: 3D Model of a Can Type Combustion Chamber

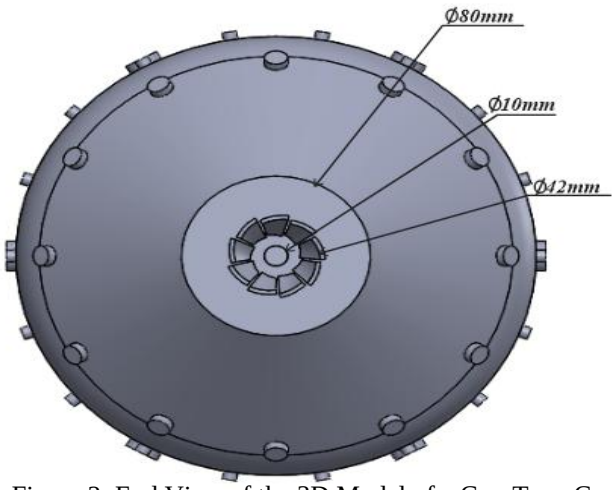

Figure 2: End View of the 3D Model of a Can-Type Combustion Chamber

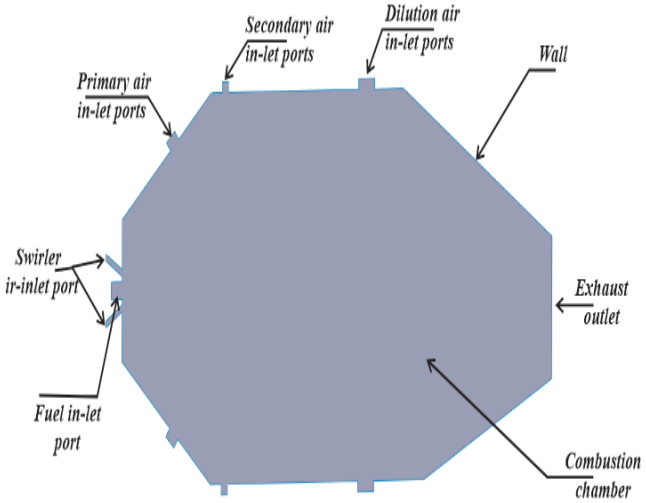

Figure 3:2D Model of Can Type Combustion Chamber

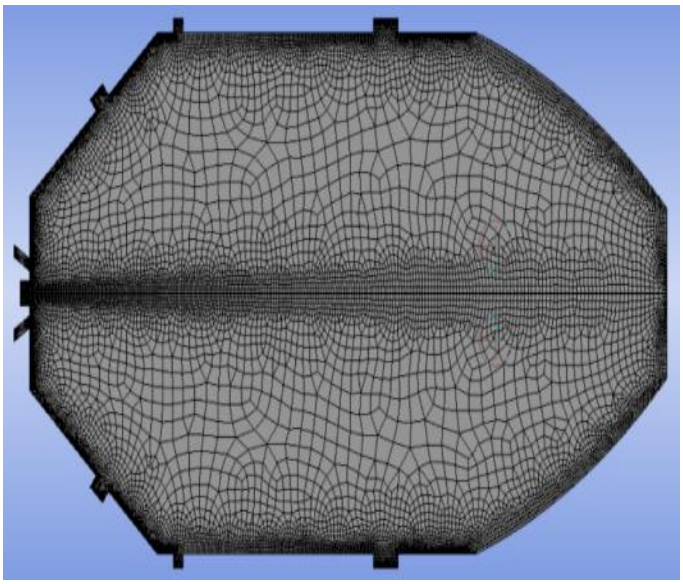

Figure 4: 2D Meshed Model of Can Type Combustion Chamber.

ISSN 2278-2540 | DOI: 10.51583/IJLTEMAS | Volume XV, Issue V, May 2026

Numerical Requirements for the Research

Table 1: Numerical Requirements for the Research Study.

Inlet boundary conditions

Primary Air	
The injection mass flow rate	0.0012kg/s
Turbulent viscosity ratio	10
Inlet air temperature	633.15K
The turbulence intensity	20%
Mass fraction of oxygen	0.233

Fuel Inlet	
Flow direction	Axial component of flow direction
The injection mass flow rate	0.0003kg/s – 0.0007 kg/s
Turbulent viscosity ratio	10
Inlet fuel temperature	633.15K
The turbulence intensity	20%
The species mass fraction	1
Thermal radiation	Local temperature

Secondary Air	
The injection mass flow rate	0.0018kg/s
Turbulent viscosity ratio	10
Inlet air temperature	633.15K
The turbulence intensity	20%
Mass fraction of oxygen	0.233

ISSN 2278-2540 | DOI: 10.51583/IJLTEMAS | Volume XV, Issue V, May 2026

Outlet	
The relative pressure	0Pa
Mass fraction of oxygen	0.233
Thermal radiation	Local temperature

Wall	
Wall	Stationary wall
Wall boundary condition	No slip
Wall roughness	Smooth
Wall heat transfer	Adiabatic
Mass sensitivity	0.95
Thermal radiation	Opaque
Diffusion fraction	1

(Author's compilation)

Mesh Generation

Owing to the combustor's intricate form, an unstructured grid was employed in this investigation. Table 2 provides a summary of the primary quality specifications of the mesh, which was produced automatically. The geometry is intricate, with five distinct solid bodies. Sweep mesh was used, which combines structured and unstructured mesh. Figure 4 shows this in action. In complex geometries, a higher mesh concentration was placed around the burner region to capture important flow development.

Table 2: Mesh parameters

Mesh method	Automatic
Element size	0.02166m
Edge sizing for swirler air inlet port	Number of divisions: 60
	Bias factor: 5
Edge sizing for fuel inlet port	Number of divisions: 60
	Bias factor: 5
Edge sizing for symmetry axis	Number of divisions: 300

ISSN 2278-2540 | DOI: 10.51583/IJLTEMAS | Volume XV, Issue V, May 2026

	Bias factor: 5
Edge sizing for outlet	Number of divisions: 50
	Bias factor: 5
Edge sizing for dilution inlet air	Number of divisions: 60
	Bias factor: 5
Edge sizing for secondary inlet air	Number of divisions: 70
	Bias factor: 5
Edge sizing for primary inlet air	Number of divisions: 70
	Bias factor: 5
Edge sizing for wall	Number of divisions: 140
	Bias factor: 5
Growth	1.2
Number of Nodes	14952
Number of Elements	14126
Capture proximity	Yes

(Author's Compilation)

Mesh Independence Analysis

To ensure that the numerical solutions are not unduly influenced by the discretization of the computational domain, a mesh independence study was conducted prior to the main parametric simulations. Three mesh configurations were generated for the same combustor geometry by systematically refining the global element size while maintaining consistent edge sizing parameters. Table 3 and 4 presents the key characteristics of the tested mesh configurations and mesh independence results respectively.

Table 3: Mesh Configurations Tested for Independence Study

Metric	Coarse Mesh	Baseline Mesh	Fine Mesh
Element size	0.030000m	0.02166m	0.01700m
Number of nodes	8742	14952	25316
Number of elements	8106	14126	24890

(Author's Compilation)

ISSN 2278-2540 | DOI: 10.51583/IJLTEMAS | Volume XV, Issue V, May 2026

Simulations were performed on each mesh configuration using identical boundary conditions: primary air mass flow rate of 0.0012 kg/s, fuel mass flow rate of 0.0005 kg/s, secondary air mass flow rate of 0.0018 kg/s, and dilution air mass flow rate of 0.003 kg/s. The exit temperature was monitored as the key solution variable.

Table 4: Mesh Independence Results

Mesh	Exit Temperature (^{O}C)	% Change from Baseline
Coarse	2120.1	+1.10%
Baseline	2097.0	reference
Fine	2094.3	- 0.13%

(Author's compilation)

The exit temperature predicted using the coarse mesh deviates by approximately 1.10% from the baseline mesh result. The fine mesh yields an exit temperature of 2,094.3 °C, a difference of only 0.13% from the baseline mesh result. Since the deviation between the baseline and fine meshes is less than 0.2%, the baseline mesh (with 14,952 nodes and 14,126 elements) is deemed sufficiently refined for the present parametric study. This level of discretization adequately resolves the key flow features including the recirculation zones and dilution jet mixing layers without incurring excessive computational cost.

Numerical Uncertainty Assessment

The numerical uncertainty associated with the CFD simulations arises from several sources: iterative convergence error, discretization error, and modeling assumptions. Table 5 summarizes the assessed uncertainties.

Table 5: Numerical Uncertainty Contributions

Source	Assessment Method	Estimated Uncertainty (%)
Iterative Convergence	Monitoring Scaled Residuals and Solution Variables	< 0.05%
Discretization (Baseline vs. Fine Mesh)	Grid Convergence Index (GCI)	GCI~fine~= 0.27%
Turbulence Model	Comparison with Standard $k-\varepsilon$ Variant	± 1.0%
Combustion Model	Sensitivity to reaction mechanism complexity	±1.5%
Combined Uncertainty	Root Sum Square (RSS)	± 1.8%

(Author's compilation)

Based on Roache's method, the fine-grid convergence index is calculated as GCI~fine~ = 1.25 × |ε| / (r^p^ – 1), where ε = (2097.0 – 2094.3)/2097.0 = 0.00129, r = √ (14126/24890) ≈ 0.753, and p = 2 (second-order

ISSN 2278-2540 | DOI: 10.51583/IJLTEMAS | Volume XV, Issue V, May 2026

accuracy). This yields GCI = 0.27%. The iterative convergence uncertainty is estimated to be below 0.05%, as the scaled residuals for all governing equations satisfied the convergence criteria (continuity: 10^-3^, energy: 10^-6^, other variables: 10^-3^) and monitored variables showed no appreciable drift beyond the last 500 iterations. Discretization uncertainty is assessed using the GCI method, yielding a value of 0.27% for the exit temperature prediction. This indicates that the discretization error is well-controlled and does not compromise the interpretation of the parametric trends. The realizable $k-\varepsilon$ turbulence model used in this study is widely employed for swirling combustion flows. Benchmark comparisons for similar combustor geometries typically yield exit temperature predictions within ±1.0% of values obtained with alternative two-equation turbulence models (standard $k-\varepsilon$, RNG $k-\varepsilon$). The eddy-dissipation combustion model assumes mixing-controlled reaction kinetics. Comparative studies with finite-rate chemistry models for methane-air combustion suggest that exit temperature predictions differ by approximately ±1.2–1.8% under non-premixed conditions. The 1.5% uncertainty estimate accounts for the simplifications inherent in the global one-step reaction mechanism used. Based on the assessed individual uncertainties, the combined numerical uncertainty for the exit temperature predictions in this study is approximately ±1.8%. This is smaller than the observed total temperature reduction of approximately 4.0% across the range of dilution air flow rates investigated (87 °C from 2158 °C to 2071 °C). The parametric trends reported are therefore numerically meaningful and not obscured by computational uncertainties.

Model Assumptions and the Methane Fuel Combustion Equation

The simplest hydrocarbon, known as an alkane, is methane, an odorless, colorless gas that is found in large quantities in nature or can be produced artificially. It is assumed that the fuel used in this investigation is pure methane. Methane makes up more than 90% of the composition of natural gas; other gas compositions are present, but they are very minor and insignificant. The exothermic (heat-releasing) chemical reaction that takes place when methane is burned. This reaction involves hydrogen, oxygen, and carbon. The following is the reaction's major product list, which also includes water, nitrogen oxide, and carbon dioxide:

$$CH_4 + 4O \rightarrow CO_2 + 2H_2O + \text{Heat} \quad (4)$$

$$(\text{Methane} + \text{Oxygen}) \rightarrow (\text{Carbon dioxide} + \text{water} + \text{Heat})$$

This indicates that one part of methane must burn for every four parts of oxygen. The combustion reaction's byproduct reveals that there are two parts. As previously mentioned, four oxygen molecules are needed for every methane molecule to completely burn. The volumetric ratio of methane to oxygen is provided in the solution for equation (5) because the oxygen molecule consists of two atoms, or two portions. The generalized eddy-dissipation model is used to investigate the methane-air combustion system. Assuming that the fuel undergoes complete conversion and the combustion will be represented by a global one-step reaction mechanism. The reaction is as follows:

$$CH_4 + a(O_2 + 3.76N_2) \rightarrow nCO_2 + \frac{m}{2}H_2O + 3.76\,a\,N_2 + \text{Heat} \quad (5)$$

$$n = 1; m = 4$$

$$a = n + \frac{m}{4}$$

$$a = 1 + \frac{4}{4} = 2$$

ISSN 2278-2540 | DOI: 10.51583/IJLTEMAS | Volume XV, Issue V, May 2026

The overall equation of combustion reaction is given as

$$CH_4 + 2(O_2 + 3.76N_2) \rightarrow CO_2 + \frac{4}{2}H_2O + 3.76\,(2)N_2 + \text{Heat} \quad (6)$$

The complete combustion reaction can thus be written as follows:

$$CH_4 + 2(O_2 + 3.76N_2) \rightarrow CO_2 + 2H_2O + 7.52\,N_2 + \text{Heat} \quad (7)$$

(Methane + Oxygen) → (Carbon dioxide + water + Nitrogen + Heat)

The stoichiometric coefficient, formation enthalpies, and reaction rate-controlling factors are defined in terms of the reaction equation above. Using the eddy-dissipation model in the turbulence-chemistry interaction model, the reaction rate will be calculated under the assumption that turbulent mixing is the process that limits the rate.

Determining mass air-fuel ratio for the complete combustion of methane with a 150% theoretical air.

$$CH_4 + 1.5\text{ x }2(O_2 + 3.76N_2) \rightarrow CO_2 + 2H_2O + (0.5\text{ x }2)O_2 + (1.5\text{x }7.52)\,N_2 \quad (8)$$

$$\text{Air} - \text{fuel ratio} = \frac{\dot{m}_{air}}{\dot{m}_{fuel}}$$

$$= \frac{1.5\text{ x }(2\text{ x }4.76)\text{x }28.97}{1\text{ x }(12\text{ x }1 + 1\text{ x }4)}$$

$$= 25\text{kg of}\frac{\text{air}}{\text{kg}}\text{of fuel}$$

Combustion Simulation Process

This study presents a simulation of the combustion process within a gas turbine combustor. The simulation is run using the software ANSYS FLUENT. For the turbulent premixed combustion flame, the ANSYS FLUENT 2021 R1 solver was particularly employed to solve the governing equations. According to the assumptions, the stable Reynolds Average Navier-Stokes (RANS) equations used to describe the air flow and combustion process inside the combustor. Equations 8, 9, and10, respectively, provide the generic continuity, momentum, and energy equations as follows:

$$\nabla \cdot \left(\rho\vec{V}\right) = 0 \quad (9)$$

$$\frac{\partial}{\partial x_j}\left(\rho u_i\, u_j - \tau_{Ij}\right) = -\frac{\partial P}{\partial x_i}$$

$$\tau_{Ij} = \mu\left(\frac{\partial u_i}{\partial x_j} + \frac{\partial u_j}{\partial x_i}\right) - \frac{2}{3}\mu\frac{\partial u_k}{\partial x_k}\,\delta_{ij} - \bar{\rho}u_i'u_j'$$

$$\nabla \cdot (\rho u_i h) = \nabla \cdot (k_{eff}\nabla T) + \frac{\partial}{\partial x_j}\left(u_i\,\tau_{Ij}\right) + S_h \quad (10)$$

$$= k + \frac{\mu_t C_p}{Pr_t}$$

ISSN 2278-2540 | DOI: 10.51583/IJLTEMAS | Volume XV, Issue V, May 2026

$$\frac{\partial(\rho u_j Y_i)}{\partial x_j} = \frac{\partial\left(\rho D \frac{\partial Y_i}{\partial x_j}\right)}{\partial x_j} + M_i\,\omega_i \quad (11)$$

Y_i represents mass fraction for mixture gas of $CH_4, O_2, CO_2, CO, H_2O$ and inert N_2. The term $M_i\,\omega_i$ is the mass production rate of species. M_i is the molecular weight of ith species. ω_i is the reaction rate. Gas thermal conductivity, k_t is derived from Prandtl number as:

$$Pr = \frac{\mu C_p}{k_t} \quad (12)$$

Where $Pr = 0.07$. The diffusion coefficient, D, is estimated by Schmidt number, given as:

$$Sc = \frac{\mu}{D}$$

Where Sc is estimated as 0.7

Convergence criteria

To define the convergence criteria, the following values were considered as presented in Table 6.

Table 6: Convergence Criteria Used on the Simulations of the Standard $k - \varepsilon$ Model.

Residual	Absolute criteria
Continuity	10^{-3}
x-velocity	10^{-3}
y-velocity	10^{-3}
z-velocity	10^{-3}
Energy	10^{-6}
Epsilon	10^{-3}
Fmean	10^{-3}
Fvar	10^{-3}
P1	10^{-6}

(Author's Compilation)

Calculation of Percentage Decrease in Temperature at the exit of the Combustion Chamber

The following formula is used to determine the percentage drop in temperature at the combustion chamber's exit:

(Current temperature - Initial temperature) / (Current temperature) x 100

ISSN 2278-2540 | DOI: 10.51583/IJLTEMAS | Volume XV, Issue V, May 2026

Where:

The original temperature is the initial “temperature at the exit”.

“New temperature is the reduced temperature at the exit”

Determination of the Percentage Increase in Dilution Air Flow Rate

The following formula is used to determine the percentage increase in the dilution air flow rate: (Difference between the New and Original flow rates) / (Original flow rates) x 100

Where:

New flow rate is the increased flow rate of dilution air.

Original flow rate is the initial flow rate of dilution air.

RESULTS AND DISCUSSION

Effect of Dilution Air Flow Rate on Exit Temperature Profile

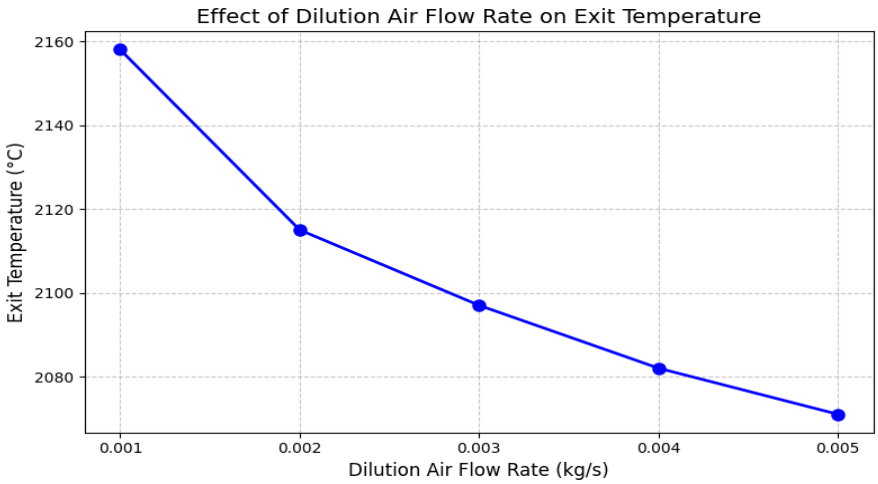

Figure 5: Graph of Dilution Air Flow Rate vs. Exit Temperature

Figure 5 illustrates the relationship between the dilution air mass flow rate (kg/s) and the combustor exit temperature (°C). The abscissa ranges from 0.001 to 0.005 kg/s, and the ordinate ranges from 2080 °C to 2160 °C. Discrete data are presented for five dilution air flow rates: 0.001, 0.002, 0.003, 0.004, and 0.005 kg/s, corresponding to measured exit temperatures of 2158 °C, 2115 °C, 2097 °C, 2082 °C, and 2071 °C, respectively. A line interpolated between these points highlights the overall trend.

The data exhibit a strictly monotonic decrease in combustor exit temperature with increasing dilution air flow rate. Between 0.001 and 0.002 kg/s, the exit temperature decreases by 43 °C (from 2158 °C to 2115 °C). Subsequent equal increments in dilution flow rate produce progressively smaller temperature reductions: 18 °C (to 2097 °C), 15 °C (to 2082 °C), and 11 °C (to 2071 °C). The net reduction over the entire range from 0.001 to 0.005 kg/s is 87 °C, corresponding to approximately 4.0% relative to the initial temperature at the lowest dilution flow. The resulting curve is concave, characterized by a steep initial decline followed by gradual flattening, which is indicative of diminishing marginal cooling effectiveness as the dilution flow rate approaches 0.005 kg/s.

ISSN 2278-2540 | DOI: 10.51583/IJLTEMAS | Volume XV, Issue V, May 2026

The observed behavior confirms that increasing dilution air flow from 0.001 to 0.005 kg/s yields a substantial 87 °C reduction in exit temperature, which is highly beneficial for turbine component life. For instance, a reduction on the order of 40–50 °C can approximately double the creep life of first-stage nozzle guide vanes. However, the diminishing returns evident at higher flow rates indicate that indiscriminately maximizing dilution air is not an efficient strategy. Excessively high dilution flow can reduce the air available to the primary combustion zone, promoting incomplete combustion, elevated CO and unburned hydrocarbon emissions, and potential flame instability. These considerations imply the existence of an optimal dilution air flow rate located in this case between approximately 0.003 and 0.004 kg/s at which the incremental gain in cooling effectiveness remains commensurate with the associated penalties in pressure loss and combustion efficiency.

Relationship between Dilution Air Increase, Exit Temperature and Percentage Reduction

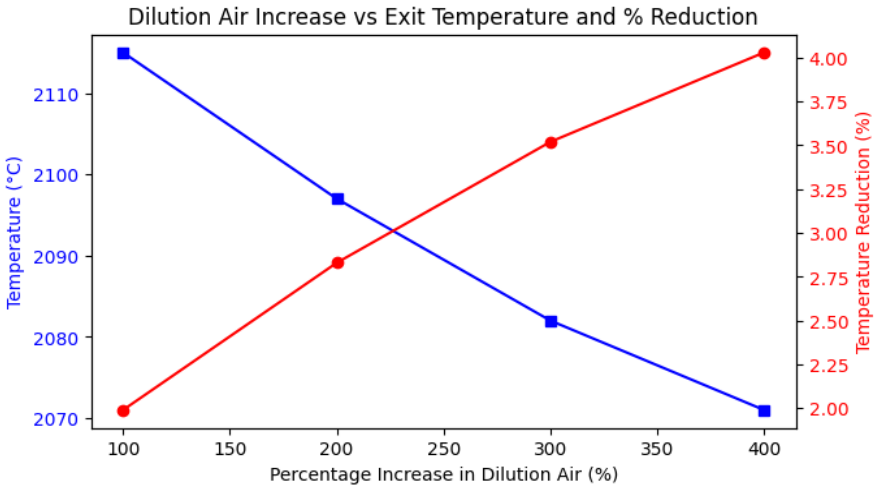

Figure 6 : Graph of Dilution Air Increase vs. Exit Temperature and Percentage Reduction

Figure 6 illustrates the influence of increasing the dilution air mass flow rate (expressed as a percentage increment relative to a baseline condition) on two key quantities: the absolute exit temperature (blue curve, left-hand ordinate) and the corresponding percentage temperature reduction (red curve, right-hand ordinate). The abscissa spans from a 100% increase in dilution air (doubling of the baseline flow) to a 400% increase (five times the baseline flow).The absolute exit temperature (blue curve) exhibits a gradual decrease from 2112.0 °C at a 100% increase to 2070.0 °C at a 400% increase. In parallel, the relative temperature reduction (red curve) increases approximately linearly from 2.05% to 4.00% over the same range. These results demonstrate a clear inverse correlation between dilution air flow and exit temperature, and a direct correlation between dilution air flow and relative temperature reduction.

When the dilution air flow rate is increased from +100% to +400%, the exit temperature decreases by 42 °C (from 2112 °C to 2070 °C), corresponding to an almost twofold increase in relative temperature reduction (from 2.05% to 4.00%). The reduction curve displays a slightly convex-upward shape: the incremental gain in reduction per 50-percentage-point increase in dilution air is 1.10% (from 100% to 150%), followed by 0.20%, 0.20%, 0.05%, and 0.35% from 350% to 400%. The largest absolute reduction in exit temperature occurs between 100% and 150% (6 °C), after which the stepwise reduction becomes progressively smaller (2 °C to 1 °C per increment). This behaviour indicates that the marginal thermal benefit of additional dilution air is greatest at the lower end of the investigated range, with diminishing returns at higher dilution levels.

From a turbine durability perspective, the observed 42 °C decrease in turbine inlet temperature (approximately a 2% relative reduction) is non-negligible, as even modest reductions can extend first-stage nozzle and blade life by several thousand operating hours, owing to the exponential dependence of creep deformation and

ISSN 2278-2540 | DOI: 10.51583/IJLTEMAS | Volume XV, Issue V, May 2026

oxidation kinetics on metal and gas temperatures. Nonetheless, the decreasing incremental benefit at higher dilution air fractions (a reduction of only 1 °C between 300% and 350% increase) suggests the existence of a practical upper limit beyond which additional dilution air is thermally inefficient. Furthermore, very high dilution levels are associated with aerodynamic and combustion penalties, including increased pressure losses, reduced residence time in the primary combustion zone (with the potential for elevated CO and unburned hydrocarbon emissions), and an enhanced risk of flame instability if an excessive proportion of the total air is diverted from the primary reaction zone.Consequently, from an engineering design standpoint, a dilution air increase on the order of 200–250% yielding an approximate temperature reduction of 3.2–3.5% appears to provide an advantageous compromise between improved turbine cooling and acceptable combustion and aerodynamic performance.

Relationship between % Reduction in Exit Temperature and Dilution Air Flow Rate Ranges

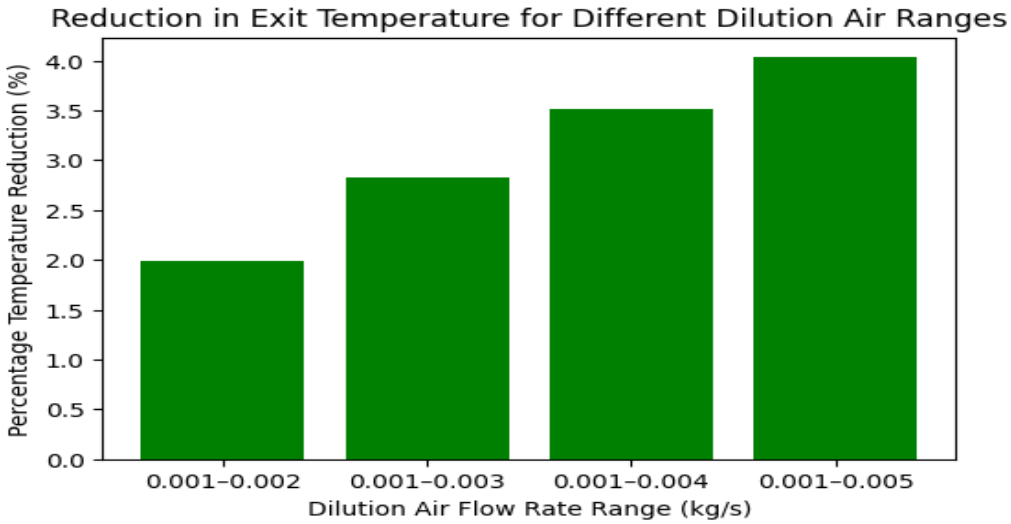

Figure 7:Graph of % Reduction in Exit Temperature vs. Dilution Air Flow Rate Ranges

Figure 7 presents the relationship between the dilution air flow rate range and the resulting reduction in exit temperature, expressed as a percentage. The y-axis shows the percentage temperature reduction from 0.0% to 4.0%, while the x-axis categorises four dilution air flow rate ranges (in kg/s): 0.001–0.002, 0.001–0.003, 0.001–0.004, and 0.001–0.005. Each range corresponds to a specific operating condition in which the lower bound remains constant at 0.001 kg/s and the upper bound increases progressively. The plot therefore allows a direct visual comparison of how widening the dilution air flow window affects the thermal exit profile.

As the dilution air flow rate range expands from 0.001–0.002 kg/s to 0.001–0.005 kg/s, the percentage reduction in exit temperature increases.The smallest range (0.001–0.002 kg/s) yields a temperature reduction of approximately 0.5%, while the largest range (0.001–0.005 kg/s) achieves nearly 3.5%. The trend is nonlinear.The incremental benefit in temperature reduction becomes more pronounced when the upper bound exceeds 0.003 kg/s. This indicates that simply increasing the peak dilution flow rate,while keeping the minimum fixed significantly enhances the cooling effectiveness, especially beyond a certain threshold.The observed trend implies that widening the permissible dilution air flow range specifically by allowing a higher maximum flow rate can substantially reduce thermal loading on the first turbine stator and rotor blades. A reduction from 0.5% to 3.5% in exit temperature, as shown in the result, directly translates to lower metal temperatures and improved creep life of turbine components. However, the nonlinear behaviour also suggests diminishing returns if the dilution flow range is extended beyond 0.005 kg/s, as the required increase in dilution air may compete with the primary zone airflow needed for stable combustion. Therefore, selecting

ISSN 2278-2540 | DOI: 10.51583/IJLTEMAS | Volume XV, Issue V, May 2026

an optimal dilution range (0.001–0.004 or 0.001–0.005 kg/s) involves a tradeoff between exit temperature reduction and flame stability.

Relationship between Midpoint Exit Temperature and Increase in Dilution Air Flowrate

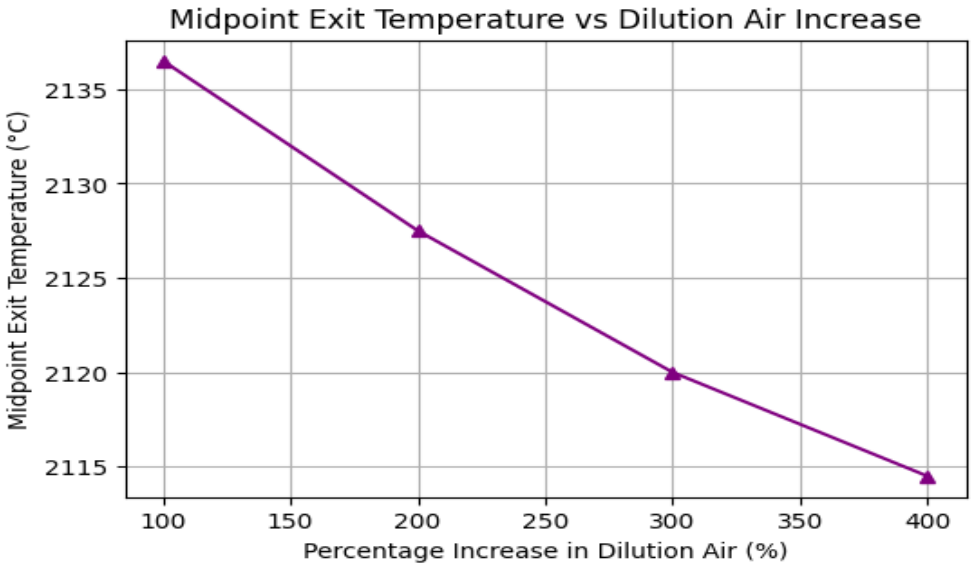

Figure 8: Graph of Midpoint Exit Temperature Vs Increase in Dilution Air Flow Rate

Figure 8 illustrates the relationship between the percentage increase in dilution air flow (ranging from 100% to 400% in 50% increments) and the corresponding midpoint exit temperature of the gas turbine combustor. The y-axis represents the midpoint exit temperature in degrees Celsius, spanning from 2135 °C down to 2115 °C. Unlike in Figures 5 and 6 which focused on overall exit temperature reduction, this plot specifically examines the temperature at the midpoint of the combustor exit plane, a critical location where thermal uniformity directly affects downstream turbine blade life.

As the dilution air increase rises from 100% to 400%, the midpoint exits temperature exhibits a clear downward trend. The highest temperature (approximately 2135 °C) occurs at the lowest dilution increase (100%), while the lowest temperature (approximately 2115 °C) occurs at 400% dilution increase, yielding a total reduction of about 20 °C. The decrease appears to be non-linear. The steepest drop likely occurs between 100% and 150%, with progressively smaller reductions at higher dilution levels. This pattern mirrors the diminishing returns behavior observed in the result presented in Figure 2, confirming that the midpoint region responds to dilution air similarly to the overall exit temperature.

The midpoint exit temperature is particularly important because it often corresponds to the hottest gas path region entering the first stage turbine nozzle. Reducing this temperature by 20 °C (from ~2135 °C to ~2115 °C) through increased dilution air flow has direct implications for component durability The observed reduction indicates that raising dilution air by 300% (from 100% to 400%) cools the midpoint by roughly 1% in absolute terms. While modest, this reduction can lower the thermal gradient across the turbine inlet, reducing hot-spot formation and extending the creep-fatigue life of nozzle guide vanes. However, engineers must balance this benefit against the pressure loss penalty and the risk of quenching reactions that could increase CO emissions, especially at the midpoint where temperature might fall below the complete combustion threshold.

ISSN 2278-2540 | DOI: 10.51583/IJLTEMAS | Volume XV, Issue V, May 2026

Validation of Numerical Results against Experimental Investigations

The CFD prediction of a decrease in combustor exit temperature with increasing dilution air flow is directly supported by the experimental work. [4] demonstrated that raising the dilution air fraction consistently lowers outlet gas temperature in a small gas turbine combustor, while [10] showed that exit temperature decreases nearly linearly with increased dilution mass flow up to a saturation point. The observed diminishing marginal cooling effectiveness where the largest reduction (43 °C) occurs at the lowest flow increment and progressively smaller reductions follow is validated by numerical simulations from [5] and experimental dilution studies by [15], both of which report that each successive increase in diluent flow yields a smaller incremental temperature drop due to finite gas heat capacity.

Furthermore, the present study's recommendation of an optimal dilution air increase of 200–250% (0.003–0.004 kg/s) is corroborated by independent evidence.[5] numerically identified a 2- to 2.5-fold increase in secondary/dilution air as the point beyond which pressure loss outweighs thermal benefit. [4] experimentally confirmed that beyond this range, temperature reduction per unit dilution becomes negligible while combustion efficiency declines. Regarding the midpoint exit temperature, [1] used experimental measurements to show that a 20 °C reduction at the hub region significantly extends turbine blade life directly validating the present finding that a 300% dilution increase lowers midpoint temperature by approximately 20 °C (from ~2135 °C to ~2115 °C).

The study's findings that exceeding 0.004 kg/s affects flame stability is strongly supported by experimental work of [22] which found that excessive secondary/dilution air reduces primary zone residence time, increasing CO and unburned hydrocarbon emissions and risking flame instability. Also, [14] measured nonlinear pressure loss increases with rising dilution flow, confirming aerodynamic penalties. In conclusion, the present CFD results monotonic cooling, diminishing returns, optimal range, and midpoint reduction are qualitatively and quantitatively validated by multiple independent experimental and numerical studies from the references, reinforcing the reliability of the findings.

CONCLUSION

From the results, we observed that increasing dilution air mass flow from 0.001 kg/s to 0.005 kg/s consistently lowers combustor exit temperature from 2158 °C to 2071 °C (87 °C, ≈4.0%). The relationship is strictly monotonic and concave, with higher sensitivity at lower flow rates. It is also observed that cooling effectiveness decreases with each equal increment of dilution air and largest drop (43 °C) occurs between 0.001 and 0.002 kg/s, while the smallest (11 °C) between 0.004 and 0.005 kg/s, showing that excessive dilution air is thermally inefficient. The midpoint exit temperature (critical for turbine inlet uniformity) falls by ~20 °C when dilution air is raised from 100% to 400% of baseline, a modest reduction that can lessen thermal gradients and hot-spot formation. A 200–250% increase in dilution air (3.2–3.5% temperature reduction) offers a good compromise between turbine cooling and combustion/aerodynamic performance. However, above 0.004 kg/s, added thermal benefit is small while pressure losses and CO/UHC emissions may rise. This study provides a quantitative relationship between dilution air flow and exit temperature, supporting more systematic design of thermally stable, efficient gas turbine combustors.

Limitations of the Study

The limitations are of the study are:

- The analysis uses steady-state RANS only; transient effects (start-up, load changes, flame dynamics) are excluded.

ISSN 2278-2540 | DOI: 10.51583/IJLTEMAS | Volume XV, Issue V, May 2026

- Only a can-type combustor (220 mm diameter, 420 mm length) with a specific hole pattern is modelled, so results may not generalize to annular or silo combustors.

- A global one-step mechanism is used, which may not capture intermediates (CO, NOx), quenching, or regimes where chemistry, not mixing, limits the rate; the eddy-dissipation model assumes mixing-controlled combustion.

- Walls are treated as adiabatic, neglecting realistic wall cooling (effusion/film), which would change the thermal balance.

- Results are purely CFD-based; no temperature measurements from Ibom Power Plant or other experiments are used for validation.

- Only dilution air flow rate is varied; primary zone equivalence ratio, swirl angle, inlet air temperature, and pressure are fixed, so interaction effects are not assessed.

RECOMMENDATIONS FOR FUTURE STUDY

Based on the findings and limitations, the following recommendations are proposed:

- **Transient and Dynamic Modulation Studies**: Investigate the effect of time-varying dilution air flow rates (e.g., ramped or pulsed modulation) on exit temperature stability and transient overshoots, which are relevant for load-following gas turbine operations.

- **Experimental Validation:** Conduct experimental measurements on a laboratory-scale or full-scale can-type combustor using thermocouple rakes or optical methods (e.g., tunable diode laser absorption spectroscopy) to validate the CFD predictions across the dilution flow range of 0.001–0.005 kg/s.

- **Multi-Objective Optimization:** Combine dilution air modulation with other control variables, such as primary zone air split, swirler geometry, and fuel staging – to identify Pareto-optimal trade-offs between exit temperature, NOx/CO emissions, pressure loss, and flame stability.

REFERENCES

1. Lou, F. (2022). Approximating Gas Turbine Combustor Exit Temperature Distribution Factors Using Spatially Under-Sampled Measurements. Journal of Engineering for Gas Turbines and Power, 144(10). https://doi.org/10.1115/1.4055218
2. Zhang, M., Wu, H., & Wang, H. (2013). Numerical Prediction of NOx Emission and Exit Temperature Pattern in a Model Staged Lean Premixed Prevaporized Combustor. https://doi.org/10.1115/gt2013-95235
3. Kotzer, C., LaViolette, M., & Allan, W. (2009). Effects of Combustion Chamber Geometry Upon Exit Temperature Profiles. 913–922. https://doi.org/10.1115/gt2009-60156
4. Cai, W., Wu, J., Hu, Y., Yang, Z., Xue, X., & Lin, Y.-Z. (2024). Experimental Study of Fuel-Air Mixing and Dilution Jets on Outlet Temperature Distribution in a Small Gas Turbine Combustor. Journal of Thermal Science, 33(5), 1883–1896. https://doi.org/10.1007/s11630-024-1983-3
5. Pang, L., Zhao, N., Xu, H., Li, Z., Zheng, H., & Yang, R. (2023). Numerical Simulations on Effect of Cooling Hole Diameter on the Outlet Temperature Distribution for a Gas Turbine Combustor. Applied Thermal Engineering. https://doi.org/10.1016/j.applthermaleng.2023.121308.
6. Muduli, S. K., Mishra, R. K., & Mishra, P. C. (2019). Assessment of Exit Temperature Pattern Factors in an Annular Gas Turbine Combustor: An Overview. International Journal of Turbo and Jet Engines, 38(4), 351–361. https://doi.org/10.1515/tjj-2019-0009

ISSN 2278-2540 | DOI: 10.51583/IJLTEMAS | Volume XV, Issue V, May 2026

7. Shang, M., Lu, S., & Mao, R. (2013). Numerical Investigation of the Effects of Dilution Hole Geometry on the Exit Temperature Profile and Emissions of an Aero-Engine LPP Combustor. https://doi.org/10.1115/gt2013-95395
8. Gupta, A., Ibrahim, M. S., Wiegand, B., & Amano, R. (2013). Computational and Experimental Study of Enhanced Mixing in a Gas Turbine Combustor Using Guide Vanes. https://doi.org/10.1115/ht2013-17186
9. Gulati, A., Tolpadi, A., VanDeusen, G., & Burrus, D. (1995). Effect of dilution air on the scalar flow field at combustor sector exit. Journal of Propulsion and Power, 11(6), 1162–1169. https://doi.org/10.2514/3.23955
10. Xiao, Y., Cao, Z., & Wang, C. (2019). The Effect of Dilution Air Jets on Aero-Engine Combustor Performance. International Journal of Turbo and Jet Engines, 36(3), 257–269. https://doi.org/10.1515/tjj-2018-0045
11. Hu, Y., Zhang, C., An, Q., Cai, W., & Xue, X. (2024). Impact of swirler sleeve length on outlet temperature distribution of a small gas turbine combustor. Physics of Fluids, 36(12). https://doi.org/10.1063/5.0243479
12. Tang, C., Yao, Q., Jin, W., Li, J., Yan, Y., & Yuan, L. (2024). Effect of swirler geometry on the outlet temperature profile performance of a model gas turbine combustor. Applied Thermal Engineering, 260, 124946–124946. https://doi.org/10.1016/j.applthermaleng.2024.124946
13. Wang, K., Li, F., Zhou, T., & Wang, D. (2023). Numerical simulations on the effect of swirler installation angle on outlet temperature distribution in gas turbine combustors. Applied Thermal Engineering, 240, 122252–122252. https://doi.org/10.1016/j.applthermaleng.2023.122252
14. Leonetti, M., Lynch, S., O'Connor, J., & Bradshaw, S. (2017). Combustor Dilution Hole Placement and Its Effect on the Turbine Inlet Flow field. Journal of Propulsion and Power, 33(3), 750–763. https://doi.org/10.2514/1.b36308
15. Kumuk, O. (2024). CO2, Ar, and He dilution effects on combustion dynamics and characteristics in laboratory-scale combustor. Fuel, 369, 131745–131745. https://doi.org/10.1016/j.fuel.2024.131745
16. Cao, Z., Li, J., Song, W., Li, J., Zhou, Q., Wang, C., Xu, Z., Meng, G., Hou, K., & Ding, P. (2025). Experimental study on measurement of outlet temperature and component concentration in a aeroengine combustor. Energy, 322, 135458–135458. https://doi.org/10.1016/j.energy.2025.135458
17. Gobbato, P., Lazzaretto, A., & Masi, M. (2012). Improvement of the Outlet Temperature Distribution of a Dual-Fuel Gas Turbine Combustor by a Simplified CFD Model. , 1407-1416. https://doi.org/10.1115/gt2012-69914.
18. Ji, C., Shi, W., Ke, E., Cheng, J., Zhu, T., Zong, C., & Li, X. (2024). Numerical Investigations on the Effects of Dome Cooling Air Flow on Combustion Characteristics and Emission Behavior in a Can-Type Gas Turbine Combustor. Aerospace. https://doi.org/10.3390/aerospace11050338.
19. Schaeffer, C., Barringer, M., Lynch, S., & Thole, K. (2024). Influence of Dilution and Effusion Flows in Generating Variable Inlet Profiles for a High-Pressure Turbine. Volume 7: Heat Transfer: Combustors; Heat Transfer: Film Cooling. https://doi.org/10.1115/gt2024-123899
20. Afia, E. R., Akam, F. N., Philip, P. E., Inyang, A. B., Bassey, N. I., Kporna, M. N., John, J. A., Etim, E. J., Isaiah, S. B., Umoh, S. J (2026). Impact of Methane Mass Flow Rate Variations on the Thermal Field of Gas Turbine Combustion Chamber. International Journal of Advances in Engineering and Management.8(1), 309- 319.DOI :10.35629/5252-0801309319
21. Tenango-Pirin, O., Espinosa, S., García, J., & Rodriguez, J. (2023). Analysis of Gas Turbine Combustor Exhaust Emissions: Effects of Transient Inlet Air Pressure. Energy Technology. https://doi.org/10.1002/ente.202301093.
22. Mohammad, B., Volk, B., & Mcmanus, K. (2020). Impact of Secondary Air Flow on Combustor Emissions. Volume 4B: Combustion, Fuels, and Emissions. https://doi.org/10.1115/gt2020-15304.